

The University of Maine

DigitalCommons@UMaine

Honors College

Spring 5-2020

In vivo Imaging of the Respiratory Burst Response to Influenza A Virus Infection

James Thomas Seuch

Follow this and additional works at: <https://digitalcommons.library.umaine.edu/honors>



Part of the [Immunology of Infectious Disease Commons](#), and the [Virus Diseases Commons](#)

This Honors Thesis is brought to you for free and open access by DigitalCommons@UMaine. It has been accepted for inclusion in Honors College by an authorized administrator of DigitalCommons@UMaine. For more information, please contact um.library.technical.services@maine.edu.

IN VIVO IMAGING OF THE RESPIRATORY BURST RESPONSE TO
INFLUENZA A VIRUS INFECTION

by

James Thomas Seuch

A Thesis Submitted in Partial Fulfilment
of the Requirements for a Degree with Honors
(Biochemistry, Molecular & Cellular Biology)

The Honors College

University of Maine

May 2020

Advisory Committee:

Benjamin King, Assistant Professor of Bioinformatics, Advisor
Edward Bernard, Lecturer in Molecular & Biomedical Sciences
Mimi Killinger, Rezendes Preceptor for the Arts in the Honors College
Melody Neely, Associate Professor of Molecular and Biomedical Sciences
Con Sullivan, Assistant Professor of Biology at University of Maine at Augusta

All Rights Reserved

James Seuch CC

ABSTRACT

The CDC estimated that seasonal influenza A virus (IAV) infections resulted in 490,600 hospitalizations and 34,200 deaths in the US in the 2018-2019 season. The long-term goal of our research is to understand how to improve innate immune responses to IAV. During IAV infection, neutrophils and macrophages initiate a respiratory burst response where reactive oxygen species (ROS) are generated to destroy the pathogen and recruit additional immune cells. While ROS molecules, such as hydrogen peroxide, help clear the virus, the signaling cascade can also lead to excess neutrophil recruitment, hyperinflammation, and tissue damage. Regulatory mechanisms that trigger over-activation of neutrophils are not understood. We are developing a zebrafish (*Danio rerio*) transgenic fluorescent reporter line to study neutrophil function and hydrogen peroxide concentration during IAV infection *in vivo*. Using Tol2 transgenesis, we are developing this line to express the hydrogen peroxide biosensor protein, HyPer, specifically in neutrophils. HyPer fluoresces at different wavelengths dependent on the concentration of hydrogen peroxide. We have designed the genetic construct to drive the expression of HyPer using the promoter of a gene highly expressed in neutrophils, myeloid peroxidase (*mpx*). Once developed, we plan to cross the line, named Tg(*mpx:HyPer*), to the neutrophil reporter line, Tg(*mpx:GFP*), and use offspring to visualize how neutrophils generate ROS in response to localized IAV infection. The Tg(*mpx:HyPer*);Tg(*mpx:GFP*) line may also be used to study neutrophil function and ROS in bacterial, fungal and other viral infections.

ACKNOWLEDGEMENTS

I would like to extend a special thanks to Dr. Benjamin King for his continuous effort as my advisor this past years and his support in this project.

I would like to thank the other members of the King laboratory for the moral support while completing this project in and out of the lab. In no particular order: Grace Smith, Lily Charpentier, Kodey Silknitter, Liz Saavedra, Kayla Barton, and Brandy Soos. I would especially like to thank Brandy Soos for her aid in the laboratory.

I would like to acknowledge the funding provided by the Genome Research Collaborative (GRC) at the University of Maine.

TABLE OF CONTENTS

INTRODUCTION	1
Threat to the Public Health	1
Influenza A Virus	2
Immunity	4
Inflammatory Response	5
Transgenic Zebrafish Models	6
METHODS	13
Re-suspending plasmids in dH ₂ O	13
Bacterial Transformations	13
Plating Bacteria	13
Overnight liquid cultures	14
Plasmid Isolation using QIAprep Spin Miniprep Kit	14
PCR amplification of the HyPer sequence	15
Fast Digestion of DNA	17
Ligation of pME-MCS and HyPer	17
qRT-PCR of genes related to oxidative burst	17
RESULTS	19
Design of a <i>Tol2</i> -compatible plasmid to express a neutrophil-specific reactive oxygen species biosensor in zebrafish.	19
5p entry clone containing the <i>mpx</i> promoter (p5E- <i>mpx</i>)	19
Middle entry clone containing the HyPer coding sequence (pME-HyPer)	23
3p entry clone containing a polyA sequence (p3E-polyA)	26

Destination vector (pDestTol2pACryGFP)	27
Predicted plasmid design	28
Expression of innate immune system genes associated with ROS	29
DISCUSSION	32
Development of the Transgenic Zebrafish Model	32
Development of the pME-HyPer entry clone from the BP reaction	33
Differential Gene Expression in Response to Infection	33
Future Applications of the Tg(<i>mpx</i> :HyPer) Zebrafish Line	35
REFERENCES	38
AUTHOR'S BIOGRAPHY	40

LIST OF FIGURES

Figure 1: The viral structure of Influenza A virus	3
Figure 2: The NADPH oxidase complex	6
Figure 3: Transgenic zebrafish model <i>Tg(MPO:mCherry)</i>	7
Figure 4: Scheme of HyPer oxidation	8
Figure 5: Neutrophils migrate to wound site following amputation of fin	9
Figure 6: Multisite Gateway Cloning	10
Figure 7: Coinjection of final <i>mpx</i> :HyPer plasmid and Tol2 transposase RNA	10
Figure 8: The forward and reverse primers for the HyPer sequence	16
Figure 9: HyPer PCR amplification protocol used with NEB Q5 Polymerase	19
Figure 10: Pairwise BLASTN alignment of p5E- <i>mpx</i>	21
Figure 11: Restriction enzyme map of <i>mpx</i> promotor region	22
Figure 12: Alignment of the p5E- <i>mpx</i> clone and Huttenlocher <i>mpx</i> promoter sequence to GRCz11 zebrafish genome	22
Figure 13: Circularized map of the predicted sequence of the p5E- <i>mpx</i> plasmid	23
Figure 14: Circularized map of the <i>actb</i> :HyPer plasmid	24
Figure 15: Pairwise BLASTN alignment of PCR amplified LR(<i>actb</i> :HyPer)	25
Figure 16: Map of the predicted sequence of the pME-HyPer plasmid	26
Figure 17: Plasmid map of 3' entry vector used in final vector assembly	27
Figure 18: Plasmid map of the pDestTol2pACryGFP destination vector	28
Figure 19: Predicted final plasmid sequence	29
Figure 20: Expression of <i>cybb</i> , <i>ncfl</i> , <i>nfe2l2a</i> , <i>serpina1</i> , and <i>sod1</i> during IAV infection from 0-120 hpi	31

LIST OF TABLES

Table 1. The Reagents used for a 50µl PCR reaction to amplify HyPer	16
Table 2. Primer sequences of attB1/attB2 sites	16
Table 3: The Oligos used for qRT-PCR to evaluate genes related to the Oxidative Burst	18
Table 4: Master mix for each gene of interest composition and reagent volumes made for (Y-1) reactions.	18

INTRODUCTION

Threat to the Public health

The World Health Organization estimates that approximately 650,000 individuals die each year due to seasonal influenza A virus (IAV) infection. Influenza vaccines are used to help prevent infection, but are often not effective because there are many strains of the virus in the general population. Trivalent and tetravalent vaccines are altered every season based on influenza strains that are predicted to spread through the population (Yamayoshi 2019). Changes in influenza strains occur through antigenic shift and antigenic drift. Antigenic shift is the accumulation of mutations in the influenza genome that result in changes in surface antigens. Antigenic shift occurs when an antigen encoding sequence of two or more unique viruses are swapped, generating a novel virus with antigens from both particles. Antigenic shift may result in the development of more virulent viral particles with a higher fatality rate, while the antigens presented may not be designated targets of the present vaccine.

New strains generated by antigenic shift are associated with influenza pandemics. There have been four pandemics in the last 100 years. The 1918 Influenza pandemic caused by a new H1N1 strain led to the deaths of approximately 50-100 million individuals worldwide (Yamayoshi 2019). The 1957-1958 Influenza pandemic was caused by a new H2N2 strain and led to 1.1 million deaths worldwide. The 1968 Influenza pandemic was caused by a new H3N2 strain and led to 1 million deaths worldwide. The 2009 Influenza pandemic was caused by H1N1 pdm09 and resulted in over 18,000 deaths (Watanabe 2010). This virus was generated through the re-assortment of antigenic sequences between

a North American swine virus and Eurasian avian-like swine virus (Yamayoshi 2019).

Influenza A Virus

IAV is a negative sense single-stranded RNA (-ssRNA) virus classified as a member of the *Orthomyxoviridae* family (Dadonaite 2019, Dou 2018, Nayak 2013). The *Orthomyxoviridae* family of viruses that have between six and eight single-stranded negative sense RNA segments. The eight RNA segments in the IAV genome that is approximately 13,500 nucleotides in length contains a total of eleven viral genes. As the segmented genome is negatively sensed, the virus relies upon the host to transcribe the -ssRNA to mRNA (+ssRNA) and then translate the mRNA to express viral proteins in order to replicate itself (Dadonaite 2019, Kwan, 2007, Watanabe 2010). Transcription and replication of the viral RNA occurs in the nucleus. The mRNA is exported from the nucleus to the cytoplasm where translation of the mRNA to protein occurs using host ribosomes (Dadonaite 2019). The eventual release of viral particles from the host cell is achieved through bud formation and scission of the plasma membrane (Dadonaite 2019, Pase 2012). While the majority of Influenza A virus particles are spherical in structure, some viral particles have been shown to be filamentous in nature (Dadonaite 2019). While we are primarily interested in the innate immune response to IAV, other types of Influenza viruses are Influenza B and C that are both within the *Orthomyxoviridae* family. The genome of Influenza B, like IAV, contains eight RNA segments, while Influenza C contains seven segments (Dadonaite 2019).

Within the lipid bilayer envelope of IAV, there are three transmembrane proteins (Dadonaite, 2019). The largest proportion of surface proteins expressed is Hemagglutinin which comprises of approximately 80% of the proteins on the viral envelope (Dadonaite

2019). The role of the 18 known Hemagglutinin variants is to interfere with the successful utilization of host produced antibodies, protecting the viral particle from immune response, as well as binding to the host cell plasma membrane (Dadonaite 2019). The second most abundant envelope protein in IAV is Neuraminidase, which has a total of 11 variants and totals approximately 17% of the transmembrane proteins. Neuraminidase binds and cleaves sialic acid receptors which is expressed on the exterior of host cell plasma membranes enabling the virus particle to enter the cell (Dadonaite 2019). Influenza virus subtypes are named based on the combination of hemagglutinin and neuraminidase antigens expressed. For example, the H1N1 subtype is hemagglutinin 1 and neuraminidase 1. The third transmembrane protein is a M2 ion channel that aids in the virus budding and scission during viral release (Figure 1) (Dadonaite 2019).

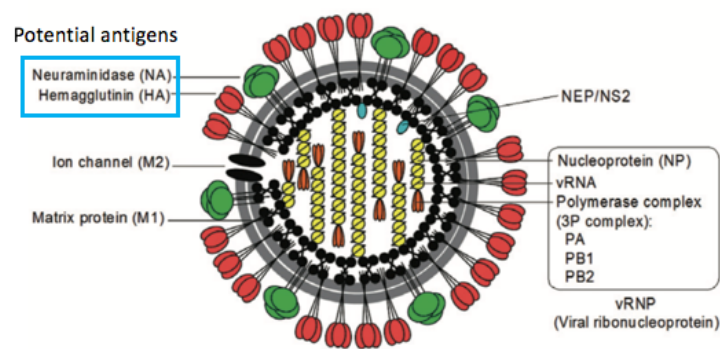


Figure 1: The viral structure of Influenza A virus. Image Adapted from: *Textbook of Influenza*, Second Edition. Edited by Robert G. et. al. 2013

Immunity

The immune system of an organism can be subdivided into the innate and adaptive immunity. Adaptive immunity is developed following initial exposure to antigen that allows for a more efficient immune response if the organism is exposed to that antigen in the future (Punt 2019). Adaptive immunity is the basis by which vaccines work. A vaccine exposes the immune system to an antigen in the form of an inert particle or protein from a pathogen prior to exposure with a live pathogen (Punt 2019). While the adaptive immune system provides a robust response to a pathogen, innate immunity provides both a defense to infection and response to injury. The innate immune system is comprised of multiple cell types include phagocytes and other cells that function as epithelial barriers to ward off pathogen entry. Phagocytes, such as neutrophils and macrophages, release chemicals used to destroy and engulf foreign particles (Punt 2019). These phagocytes develop from a common myeloid progenitor found in bone marrow (Punt 2019).

Following infection by a pathogen, cytokines are released into the circulatory system to signal the presence of damage and/or foreign particles. Cytokines, such as $\text{TNF}\alpha$, and $\text{IL-1}\beta$, promote an inflammatory response and recruit immune cells through chemotaxis (Punt 2019). Vasoactive factors released near the site of infection increases local blood flow, and capillary permeability to allow leukocytes to migrate to the site of infection (Pase 2012, Punt 2019). The majority of immune cells that migrate to the site of infection are macrophages and neutrophils to clear the infection. Both cell types are capable of producing an oxidative burst, where reactive oxygen species are released to destroy phagocytosed particles, and act as a cell signaling particle (Pase 2012, Punt 2019, Yoo 2011).

Inflammatory response

The response by the innate immune system to infection and/or injury is a dynamic process where signaling cascades control the expression of genes. Reactive oxygen species (ROS) is an important signaling molecule during an inflammatory response (Punt 2019, Panday 2015, Niethammer 2009). ROS molecules and their intermediates, such as hydrogen peroxide (H_2O_2) and hypochlorite, also function to degrade deceased cells, pathogens, and foreign particles (Pase 2012, Punt 2019). However, these molecules do not discriminate between their designated targets and the surrounding tissue of the organism (Punt 2019). ROS can cause damage to the surrounding tissues. As such, the processes relating to ROS containing molecules must be tightly regulated to enable an effective response without negatively impacting the health of the organism (Pase 2012).

ROS are generated in cells by the NADPH oxidase (NOX) complex (Figure 2) (Punt 2019, Panday 2015). In the zebrafish, the primary protein in this NOX complex is *cybb*. The cytosolic subunit of the NOX complex, named P47, is encoded by the neutrophil cytosolic factor 1 (*ncf1*). P47 is an important activator of the NOX complex. Once the complex is activated, it is translocated to the membrane (Panday 2015). Another regulator of ROS is *nfe2l2a*, a transcription factor used to regulate the transcription of antioxidant proteins that protect tissues from damage. Expression of the *serpinal* gene is regulated by *nfe2l2a* transcription factor, and functions to reduce damage to surrounding tissues from inflammatory enzymes. The expression of superoxide dismutase 1 (*sod1*) is also regulated by *nfe2l2a*, and is used to render superoxide inert. All of these genes function as part of the dynamic response to pathogen infection.

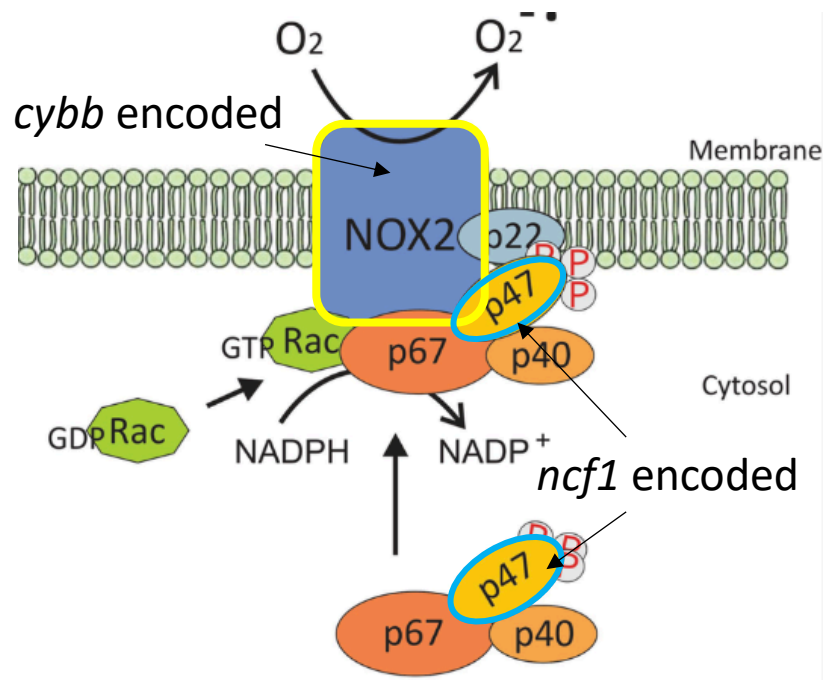


Figure 2: The NADPH oxidase complex generates radical oxygen molecules to develop reactive oxygen species containing molecules for use in the respiratory burst response. Image adapted from Gonzalez-Perilli L et al. (2019).

If the oxidative burst is not carefully regulated, a hyperinflammation may occur. Hyperinflammation occurs when ROS generated by the response to infection recruit and activate additional phagocytes to the site of infection. It is known that the signaling from ROS particles recruit additional neutrophils to the site of infection (Yoo 2011). The additional neutrophils further promote an oxidative burst cascade. We believe that a hyperinflammatory response to an influenza A virus infection correlates with neutrophil density and the activity of the respiratory burst response.

Transgenic Zebrafish Models

The zebrafish is useful vertebrate model to study the mechanisms of human disease *in vivo*. Zebrafish can be easily grown on larger scales and less expensively than mammalian models allowing for larger sample sizes (Yoo 2011). Zebrafish embryos are

transparent for up to five days post fertilization and enables *in vivo* observations using microscopy (Yoo 2011). Zebrafish embryos develop ex utero, and can be collected at single cell stage. At the single cell stage, a microinjection can be used to make a transgenic zebrafish line by injecting a plasmid, or a morphant by injecting an antisense morpholino. Transgenic zebrafish lines are used to model diseases in several ways. One example is the WHIM (*Tg1(-8mpx:cxc4b-EGFP)*) model that overexpresses a transgene that has a truncated *cxc4b* gene that impairs neutrophil function. Another example are fluorescent reporter lines that can be used to visualize individual cell types *in vivo* using fluorescent reporter molecules like green fluorescent protein (GFP) (Pase 2012) (Figure 3). Fluorescent reporter zebrafish lines used study neutrophil migration include the *Tg(mpx:GFP)* and *Tg(mpx:Dendra2)* zebrafish lines (Yoo 2011). To expand available zebrafish models of innate immune responses, this project sought to generate a zebrafish line in which neutrophils express a ROS biosensor.

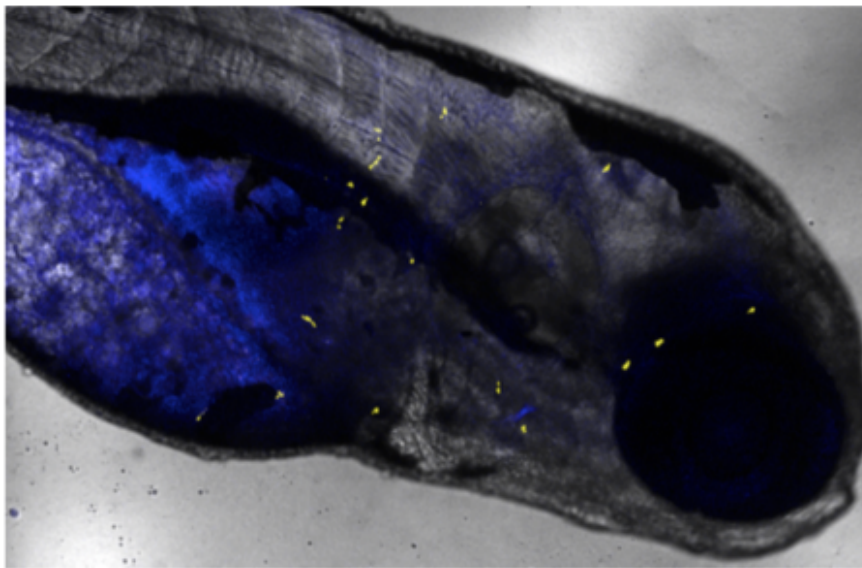


Figure 3: Transgenic zebrafish model *Tg(MPO:mCherry)*, with MA-eCFP-PR8 color-flu injected into swimbladder. The neutrophils are shown in green, and the IAV fluoresces blue.

The HyPer protein was engineered to be a ROS biosensor, with fluorescence activity dependent on the concentration of ROS molecules (Panday 2015). This protein was developed by inserting the a circularly permuted yellow fluorescent protein (YFP) into the *E. coli* OxyR H₂O₂ sensing protein (Belousov 2006). Following oxidation of Cys199 from hydrogen peroxide, Cys199 and Cys208 form a disulfide bond resulting in conformational changes in OxyR residues 205-222 (Figure 4) (Belousov 2006) As OxyR is a prokaryotic protein, there should be no interactions with intracellular signaling in eukaryotic cells (Belousov 2006). The presence of this protein product in locally damaged tissue, or near the site of infection allow for the detection of H₂O₂ (Panday 2015). H₂O₂ is predominantly produced by neutrophils and other granulocytes. The Tg(*lyz*:Hyper) model use the Lysozyme C (*lysc*) promotor to express HyPer in neutrophils allowing visualization of the H₂O₂ concentration at a wound site (Panday 2015, Pase 2012) (Figure 5).

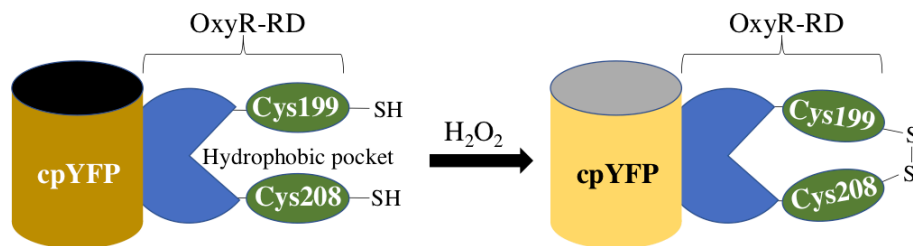


Figure 4: Scheme of HyPer oxidation resulting from hydrogen peroxide exposure. Residues Cys199 and Cys208 of the OxyR protein generate a disulfide bond resulting in conformational changes of the regulatory domain of OxyR. Figure developed with information provided in Belousov 2006, Bilan 2018.

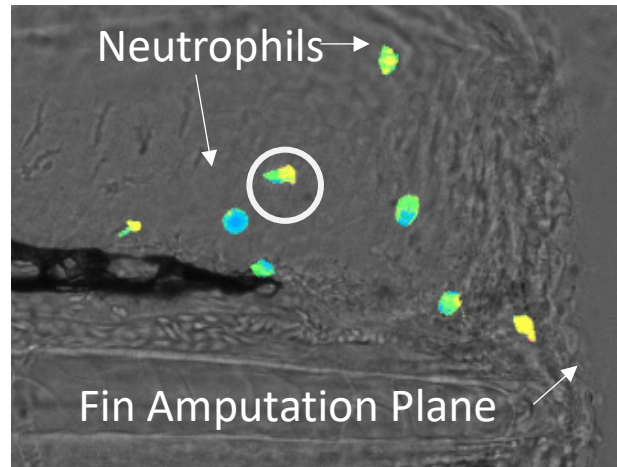


Figure 5: Neutrophils of the Tg(lyz:HyPer) zebrafish model migrate to wound site following amputation of fin. Image taken 59.5 minutes post amputation. The detected fluorescence transitions from blue to yellow in the presence of hydrogen peroxide. The Neutrophil denoted in the white circle shows the transition from green to yellow indicating an increasing concentration of hydrogen peroxide. Image adapted from Pase 2012.

Multisite Gateway Cloning is used to generate complex plasmid vectors for use in transgenesis that are constructed using multiple entry vectors. The LR Clonase reaction using the *att* site recombination system of lambda phage (Kwan 2007). Using *attR* and *attL* sequences in the entry vectors, the vectors are cloned into the destination vector in a designated order. The 5p entry clone contains the promoter element of interest with flanking *attL4/R1* sites (Kwan 2007). The middle entry vector contains the coding sequence of interest, e.g. the coding sequence of a reporter like HyPer, flanked by *attL1/L2* sequences. The 3p entry vector most often contains a polyadenylation (polyA) signal (Kwan 2007). The final plasmid vector is coinjected into a single cell zebrafish embryo with Tol2 transposase RNA to generate founders of a transgenic line (Figure 7). The multisite Gateway Cloning system has successfully been used in zebrafish to make several zebrafish lines (Kawakami 2007).

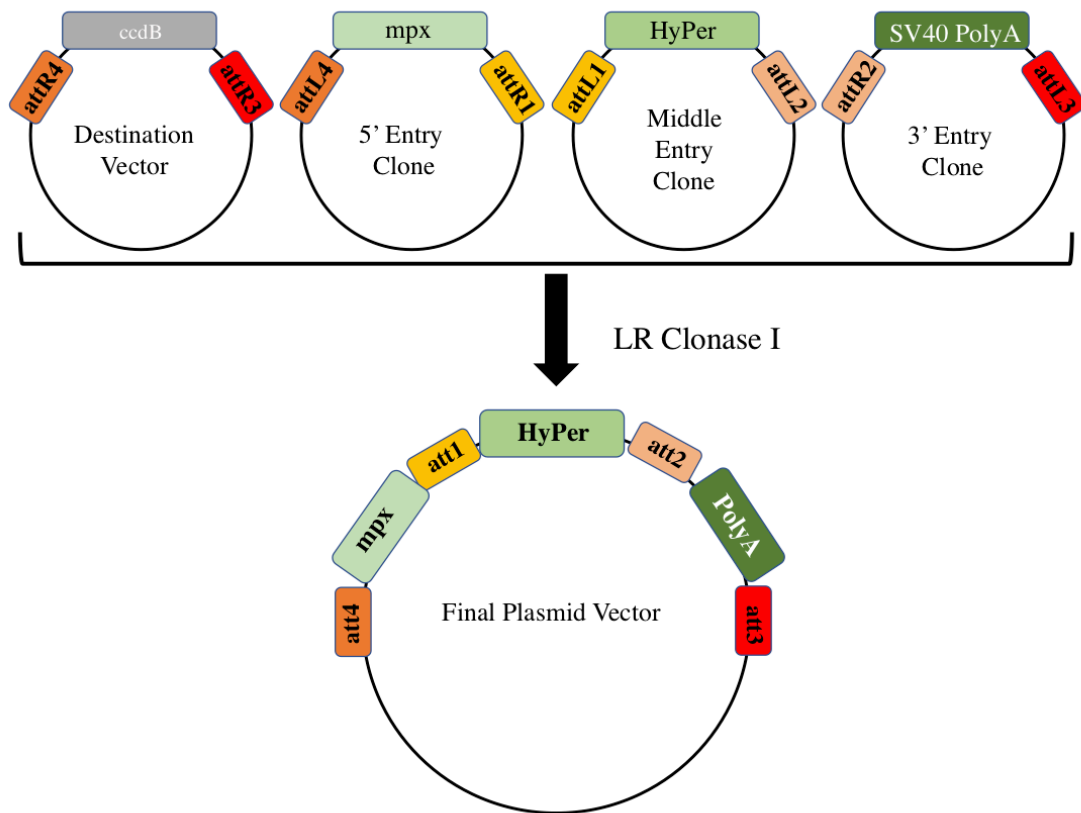


Figure 6: Multisite Gateway Cloning. Scheme of LR reaction of three entry vectors using LR Clonase I.

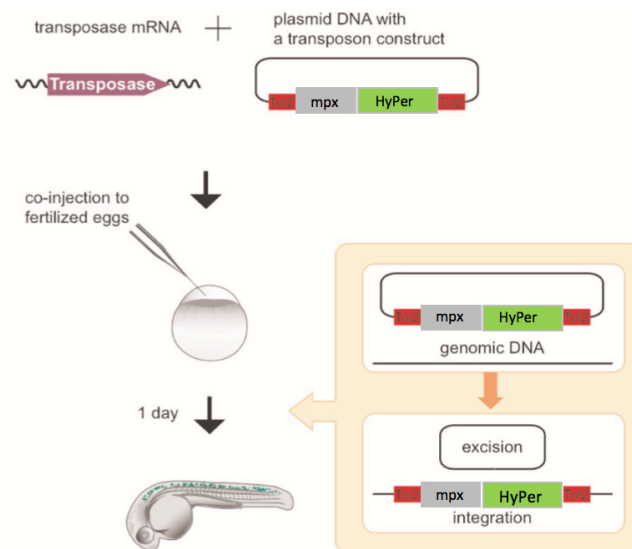


Figure 7: Coinjection of final *mpx:HyPer* plasmid and Tol2 transposase RNA. Image adapted from Kawakami, 2007.

The long-term goal of this project was to create a transgenic zebrafish line that would express HyPer specifically in neutrophils. In multisite Gateway Cloning, expression of the reporter gene is driven by a promoter for a gene that is specific to the cell type of interest. In several zebrafish neutrophil reporter lines, the promoter for myeloid-specific peroxidase (*mpx*) was used (Yoo 2011). This enzyme is expressed in neutrophils, and plays a role in the formation of reactive oxygen intermediates (Yoo 2011). A 5p entry clone containing the *mpx* promoter was Jeremy Charette, a former graduate student in Prof. Carol Kim's Lab at the University of Maine. The HyPer coding sequence used was obtained from a *actb*:HyPer plasmid given to Prof. King's Lab by Prof. Philipp Niethammer at Memorial Sloan Kettering Cancer Center (Niethammer 2009). This plasmid contained a promoter for beta actin, a gene expressed in most cell types, followed by the HyPer sequence. Following PCR amplification, we worked to clone that HyPer coding sequence into pME-MCS using a BP Clonase II reaction.

Using a LR reaction, the final plasmid vector would be assembled using the 5p-entry, middle-entry, and 3p-entry clone into the destination vector, pDestTol2pACryGFP (Berger 2013). This destination vector contains an alpha-crystallin promoter preceding a GFP sequence to enable screening of zebrafish at 2 days post fertilization to detect successful transgenesis. The 5p entry vector, p5E-*mpx*, contains the *mpx* promoter. The middle entry vector, pME-HyPer, would contain the HyPer coding sequence successfully cloned into pME-MCS. The third plasmid to be used in the final vector assembly was p3E-polyA. Following the successful cloning of HyPer into the middle entry vector, the three sequences would have been combined in the Tol2 plasmid destination vector, to generate the *mpx*:HyPer plasmid.

The Tg(*mpx*:HyPer) model we worked towards generating would be useful to characterize concentrations of H₂O₂ in neutrophils *in vivo* following infection or injury. This would be a powerful tool to further understand innate immunity and inflammatory responses to infection (Yoo 2011). This model would also help us understand hyperinflammatory responses. These responses can lead to tissue damage following excess neutrophil recruitment and ROS production. The model, Tg(*mpx*:HyPer), would enable us to use fluorescent microscopy to observe both events.

METHODS

Re-suspending plasmids in dH₂O

Plasmids from the Tol2 kit were resuspended in molecular grade DNase/RNase free water. The lab workbench was sprayed with ethanol prior to removal of plasmids from Tol2 kit packaging. Scissors were sprayed with ethanol prior to excising the plasmid containing filter paper for each plasmid. Sterile forceps were used to place each excised filter paper into 1.5 ml microcentrifuge tubes that were pre-labeled. When resuspending the plasmid, 50 µL of DNase/RNase free water was added to the tube.

Bacterial Transformations

Tubes containing plasmid and 10-beta competent *E. coli* (New England Biolabs, Ipswich, MA) were defrosted on ice. Once defrosted, 1 µl of plasmid was added to the bacteria. Solution was lightly mixed and incubated for 30 minutes on ice. The bacteria solution warmed to 42°C for 30 seconds and incubated for 5 minutes on ice. Following incubation, 925 µl of 10-Beta/Stable Outgrowth Media (New England Biolabs, Ipswich, MA) was warmed to 37 °C added to solution. Bacterial solution was incubated at 37°C for 60-75 minutes on a shaking incubator set at 225 rpm.

Plating Bacteria:

To generate 9 plates to culture the bacteria, 3.75 g of agar and 6.25 g of Luria Broth (LB) was added to 250 ml of dH₂O. The solution was then autoclaved. While agar solution was cooling on a stir plate, 125 µl of 1000X antibiotic stock (Ampicillin or Kanamycin) was added. The plates are then poured, and cooled in a 37°C incubator.

Following the final incubation in the transformation protocol, bacteria were plated.

Bacteria were plated with differing volumes ranging from 50 µl, 100 µl, 150 µl using a sterile cell spreader. The plates with are incubated overnight at 37°C, while unused plates are stored in a 4°C refrigerator.

Overnight liquid cultures:

For each colony of interest that grew on a plate, 7 ml of LB media was added to sterile glass tubes. 3.5 µl of antibiotic stock was added to each tube, and lightly mixed by vortexing. Volumes of Kanamycin and/or Ampicillin stock may vary depending on previously noted bacterial survival. A single sterile loop was used to transfer the bacterial colony from a plate to the appropriately labeled liquid culture. The liquid cultures were incubated at 37°C overnight on a shaking incubator set at 180 rpm.

Plasmid Isolation using QIAprep Spin Miniprep Kit:

Following an overnight incubation period, 500 µl of liquid culture was combined with a glycerol solution in a freezer tube generating a glycerol stock. 1.4 ml of liquid culture was centrifuged at 2 rcf (relative centrifugal field) for 3 minutes at 18°C. The supernatant was discarded in a bleach solution. This process was repeated until the entirety of the liquid culture was pelleted. The pellet of bacteria was resuspended in 250 µl of P1 Buffer. 250 µl of LyseBlue lysis reagent and Buffer P2, was added to the microcentrifuge tube. The solutions were mixed through 4-6 inversions of the tube. Following an incubation at room temperature for 5 minutes, 350 µl of Buffer N3 was added to the sample and was mixed via inversions 4-6 times until the solution became clear. The sample was centrifuged for

10 minutes at 10,000 rpm. 800 µl of the resulting supernatant was added to a QIAprep 2.0 spin column. Flow-through following a 60 second centrifugation was discarded. The column was washed for 60 seconds at 13,000 rpm with 500 µl of BufferPB, and the supernatant was discarded. The column was washed for 60 seconds at 13,000 rpm with 750 µl of BufferPE, and the supernatant was discarded. The column was dried by an additional 60 second 13,000 rpm centrifugation. The column was placed in a 1.5 ml microcentrifuge tube. DNA was eluted with 30µl of DNase/RNase free water. Plasmid concentration and purity was evaluated using a NanoDrop OneC spectrophotometer (Thermo Scientific Fisher, Waltham, MA).

PCR amplification of the HyPer sequence:

PCR amplification of HyPer was performed using New England Biolabs (NEB) Q5 High-Fidelity DNA Polymerase following the manufacturer's protocol (Table 1.) The primers used were designed to amplify a HyPer sequence containing restriction sites to be used in restriction digests enabling the development of pME-HyPer from a BP Clonase II reaction (Figure 8). When the ligation of the BP reaction yielded poor results, primers were redesigned with the attB1, and attB2 sites (Table 2.). The PCR protocol used 35 cycles for DNA amplification, using the temperatures recommended from NEB (Figure 9).

Table 1. The Reagents used for a 50 μ l PCR reaction to amplify HyPer.

Reagent(s)	Volume (50 μ l reaction)
5X Q5 Reaction Buffer	10 μ l
10 mM dNTPs	1 μ l
10 μ M Primers (F +R)	5 μ l
Template DNA	Final concentration <1,000ng
5X Q5 High GC Enhancer	10 μ l
Q5 High-Fidelity DNA Polymerase	0.5 μ l
Nuclease Free Water	Volume to 50 μ l

HyPer Primer Sequence(s)	
Forward	5' – AGAAGA GGATCC CACC ATGGAGATGGCAAGC – 3'
Reverse	3' – TCTTCT CTTAAG TTAAACCGCCTGTTT A – 5'

Figure 8: The forward and reverse primers for the HyPer sequence. The CACC highlighted in the blue box is the Kozak sequence. The BamH1 restriction site is highlighted in the yellow box, and the EcoR1 restriction site is in the purple box. The sequences highlighted in the green box are complementary to the HyPer coding sequence.

Table 2. Primer sequences of attB1/attB2 sites.

attB1/attB2 Primer Sequence(s)	
Forward	5' – TCAAGTTTGTACAAAAAAGCAGGCTCGATGGAGATGG CAAGCCAGCAG – 3'
Reverse	3' – CCCCACTTTGTACAAGAAAGCTGGGTGTTAAACCGCCTGT – 3'

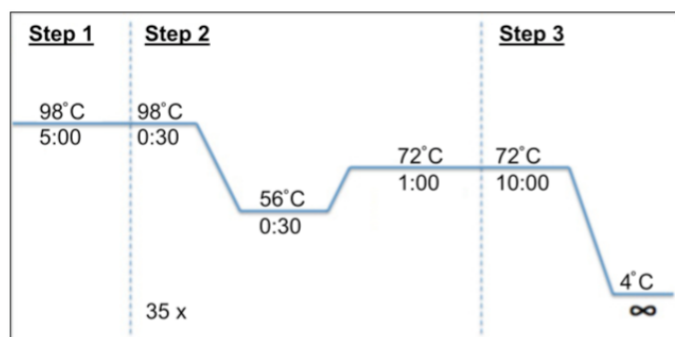


Figure 9: HyPer PCR amplification protocol used with NEB Q5 Polymerase.

Fast Digestion of DNA:

To digest the unpurified HyPer PCR product, a Fast digestion protocol from Thermo Fisher Scientific was used. A 30 µl reaction was set up using 2 µl of 10X FastDigest buffer, approximately 2 µg of DNA, 0.5 µl of EcoR1, 0.5 µl of BamH1, and 25 µl nuclease free water to total volume. This solution was incubated at 37°C for 30 minutes. The enzymes were inactivated at 65°C for 20 seconds.

Ligation of pME-MCS and HyPer:

To ligate the HyPer plasmid fragment in a 100 ng reaction, 2 µl of pME-MCS plasmid was added into a 1.5 ml microcentrifuge tube. 2 µl of T4 ligation buffer was added to the tube. HyPer digestion was added to the microcentrifuge tube with variable volumes to achieve a final concentration of 50 ng/µl. Molecular grade water was applied to bring the total volume to 19 µl. T4 ligase was added to the tube with a volume of 1 µl. The sample was incubated overnight at 4°C

qRT-PCR of Genes Related to Oxidative Burst

If needed, oligos were re-suspend to a 100 µM concentration for each of the genes being evaluated. For each pair of oligos, 5 µl of the forward and reverse oligos were mixed with 90µl of nuclease free water in a 1.5 ml microcentrifuge tube (Table 3). Bio-Rad SsoAdvanced Universal SYBR Green Supermix (Bio-Rad, Hercules, CA), nuclease free water and oligo solution was generated (Table 4). To each appropriate well on a Bio-Rad qPCR plate, 9 µl of master mix was added. To each appropriate well, 1 µl of the sample cDNA was added to the well. The plate was covered with a Bio-Rad plate adhesive film.

The sealed plate was vortexed lightly to mix the master mix and cDNA. The plate was placed in the Bio-Rad CFX96 plate, and the software of the qRT-PCR program was run to determine threshold cycle (C_t) values for each sample. Fold changes were calculated using the $\Delta\Delta C_t$ method.

Table 3: The Oligos used for qRT-PCR to evaluate genes related to the Oxidative Burst

qRT-PCR Oligos		
Gene Symbol	Sequence Forward	Sequence Reverse
<i>serpina1</i>	AAGCTCTGTGGACCTGTTTATG	CATGGTGCTGTCCTCTACAATC
<i>sod1</i>	CTCTGTCAGGCCAACATTCTAT	GTAATTGTCAGCGGGCTAAGT
<i>actb</i>	GATCTGGCATCACACCTTCTAC	CACCAGAGTCCATCACAATACC
<i>nfe2l2a</i>	TGTCCTTCCTCCTTCTCTCTT	CGTCGATGTTTATTGCCTCTTTAC
<i>ncf1</i>	CAGCTCATTCGGGACTTCTT	GTTCTCTCTGTTTGTCTCCTC
<i>cybb</i>	CCTGGGAGGACTTTCACCTTC	CTTGTGCTGTCTGCCTAGTT

Table 4: Master mix for each gene of interest composition and reagent volumes made for (Y-1) reactions.

Reagent	Volume	Example ($Y=7$)
SYBR Green	$5\mu\text{l} \times Y$	$5\mu\text{l} \times 7 = 35\mu\text{l}$
Nuclease-free water	$3.5\mu\text{l} \times Y$	$3.5\mu\text{l} \times 7 = 24.5\mu\text{l}$
Forward + Reverse oligos	$0.5\mu\text{l} \times Y$	$0.5\mu\text{l} \times 7 = 3.5\mu\text{l}$

RESULTS

Design of a *Tol2*-compatible plasmid to express a neutrophil-specific reactive oxygen species biosensor in zebrafish.

A *Tol2*-compatible expression plasmid was designed to generate a stable transgenic zebrafish line to express HyPer specifically in neutrophils. The overall plasmid design was based on multisite Gateway cloning that assembles three entry clones and a *Tol2*-based destination vector. The three entry clones assemble into a construct that includes a promoter sequence to initiate transcription in the cells of interest, coding sequence of the reporter protein, and poly-adenylated (polyA) tail for transcription termination. In Gateway cloning technology, the three entry clones are named the 5p entry (p5E), middle-entry (pME), and 3p-entry (p3E) clones, respectively. For this design, the p5E clone included the promoter for the myeloid peroxidase (*mpx*) gene, a gene that is highly expressed in neutrophils. This clone was named p5E-*mpx*. The pME clone was designed to contain the coding sequence for HyPer. This clone was named pME-HyPer. The p3E clone contained the polyA tail and named p3E-polyA. The destination vector used in our design, named pDestTol2pACryGFP, expresses GFP using an alpha-crystallin promoter that can be used to screen transgenic embryos by lens fluorescence. The following sections describe the three entry clones, destination vector, and the final plasmid design in more detail.

5p entry clone containing the *mpx* promoter (p5E-*mpx*)

In order to develop the transgenic line, a 5p entry clone that contained the *mpx* promoter in order to drive expression of HyPer specifically in neutrophils was used. This p5E-*mpx* clone was created by Jeremy Charette, a former graduate student in Prof. Carol

Kim's Laboratory at the University of Maine. Colonies of this clone were grown with 10B-*E. coli* and a portion of the *mpx* promoter from the clone was sequenced. The sequence contained the first intron that was 345 bp long, the first exon that was 135 bp long, and 353 bp upstream of the first exon (Figure 10). This sequence was only a portion of the *mpx* promoter in the p5E-*mpx* clone and additional sequencing needs to be performed to completely verify the promoter in the p5E-*mpx* clone. This sequence also matched a portion of the *mpx* promoter that was used in the Tg(*mpx*:EGFP) zebrafish neutrophil fluorescent reporter line developed by Prof. Anna Huttenlocher's Laboratory at the University of Wisconsin (Freisnger 2014). In this line, the *mpx* promoter drives the expression of enhanced green fluorescent protein (EGFP) in neutrophils and is used by our laboratory and others worldwide to visualize neutrophils in embryos using confocal imaging (Figure 3). The Tg(*mpx*:EGFP) line uses a *mpx* promoter that is 8,177 bp in length (Figure 11). The *mpx* promoter sequence was derived by taking 10,000 bp upstream of *mpx* in the GRCz11 zebrafish genome assembly and looking for the fragment between the *Choi* and *XhoI* restriction enzyme cut sites described in Prof. Huttenlocher's paper. This promoter sequence contained the first exon, the first intron, and 7,082 bp upstream of the first exon. However, the sequence did not align adjacent to the beginning of the second exon as the p5E-*mpx* clone sequence did (Figure 12). Since a complete sequence for the p5E-*mpx* clone was not generated, the p5E-*mpx* clone sequence was merged with the 7,092 bp sequence. The resulting sequence was used as the *mpx* promoter sequence in the p5E-*mpx* clone for the purposes of designing the *mpx*:HyPer plasmid. Using the predicted *mpx* promoter sequence, we made a sequence map for the 8,341 bp p5E-*mpx* clone that will be

used as the 5p entry vector to develop the Tg(*mpx*:HyPer) transgenic zebrafish line (Figure 13).

Query	277	ATCCCTAAAAACACATATTGAGACATTTATAGAGTAAACACATAACATGCATTGTTTATG	336
Sbjct	7785540	ATCTCTAAAAACACATATTGAGACATTTATAGAGTAAACACATAACATGCATTGTTTATG	7785599
Query	337	AATAGTAACAATAGTACATAAAATGTACTGCTTATGCAGAAAATGTGTTAAATGTGTGAA	396
Sbjct	7785600	AATAGTAACAATAGTACATAAAATGTACTGCTTATGCAGAAAATGTGTTAAATGTGTGAA	7785659
Query	397	AATATTATACAAGGTTTATAAATGTTATAAAATTTTAAAGATAATATCGATGGATTT	456
Sbjct	7785660	AATATTATACAAGGTTTATAAATGTTATAAAATTTTAAAGATAATATCGATGGATTT	7785719
Query	457	AAACACAATTTTAAAACTAGTCAAATGTCTGTTAAATTTTGCAGTAAATCCACTAAAAAT	516
Sbjct	7785720	AAACACAATTTTAAAACTAGTCAAATGTCTGTTAAATTTTGCAGTAAATCCACTAAAAAT	7785779
Query	517	GTGTTTGCATTGCAATCAGCACCACACAGATAAACCATTAACAGCATTTAATCATGCAAT	576
Sbjct	7785780	GTGTTTGCATTGCAATCAGCACCACACAGATAAACCATTAACAGCATTTAATCATGCAAT	7785839
Query	577	CAAATTATGAAAAATAAAAAAGTTTCAAATAGCatttttttACCAGTAAACATGCG	636
Sbjct	7785840	CAAATTATGAAAAATAAAAAAGTTTCAAATAGCATTTTTTTACCAGTAAACATGCG	7785899
Query	637	TGTCTCAGGCTCACTGGTTCTGGACTTGAAGCTCAGAGTAAGTTGTGCTGAATGTATGCA	696
Sbjct	7785900	TGTCTCAGGCTCACTGGTTCTGGACTTGAAGCTCAGAGTAAGTTGTGCTGAATGTATGCA	7785959
Query	697	GCGGCTGCTCTTTTAAACCATCCCTCATCTTTAGTCTGCTGAGCATCATTGGGGGAGTT	756
Sbjct	7785960	GCGGCTGCTCTTTTAAACCATCCCTCATCTTTAGTCTGCTGAGCATCATT-GGGGGAGTT	7786018
Query	757	TCTGGTGGTTTACTTCCTTTTTCCTTTTCATTACCATATGTGGTGCTTATTTATTGAT	816
Sbjct	7786019	TCTGGTGGTTTACTTCCTTTTTCCTTTTCATTACCATATGTGGTGCTTATTTATTGAT	7786078
Query	817	TTATTGAAGTTGACAATCTGACATTCACTCATCCAGACTCAACATTACAGGAATTC	876
Sbjct	7786079	TTATTGAAGTTGACAATCTGACATTCACTCATCCAGACTCAACATTACAGGAATTC	7786138
Query	877	ATATGCACACaaaaaaaTCATACCATTAAAATGAAAGATTGCACATGTTTCACCTT	936
Sbjct	7786139	ATATGCACAC-AAAAAAAATCATACCA-TTAAATGAAAGATTGCACATGTTTCACC-T	7786195
Query	937	TTAAATAAAACGATTGAGATCATAATTTGAGTAAGTGCTTTTGTAGAATACAATTAC	996
Sbjct	7786196	TTAAATAAAACGATTGAGATCAT-ATTGGAGTAAGTGTC-TTTGTAG-ATACA--TTAC	7786250
Query	997	-AGTCTAG--TTATCTATTATTATTATTTCATTAG-ATGATCAACATATTAGTGG	1052
Sbjct	7786251	AAGCTAGTTTATCTATTATTATTATTAAATAAGAATGATCAACATATTAGTGG	7786310
Query	1053	TTCAAGTGTAATATAATCGAAACGCTTCTCCAGCTTCTTTTAT-GCATGGCCTGAACA	1111
Sbjct	7786311	TCAAAGTGTAATATATAAGGAAACGGTCTTTCAAGTCTTTTATGGCATTGCC-GAAAA	7786369
Query	1112	AGAA 1115	
Sbjct	7786370	AAAA 7786373	

Figure 10: Pairwise BLASTN alignment of a 1,144 bp sequence of a fragment of the p5E-*mpx* clone and Chr. 10 from the GRCz11 zebrafish assembly. The coordinates of exon 1 for *mpx* are from Chr. 10: 7,785,885-7,786,020 in reverse orientation (highlighted in blue). The alignment was 96% identical over 844 bp.

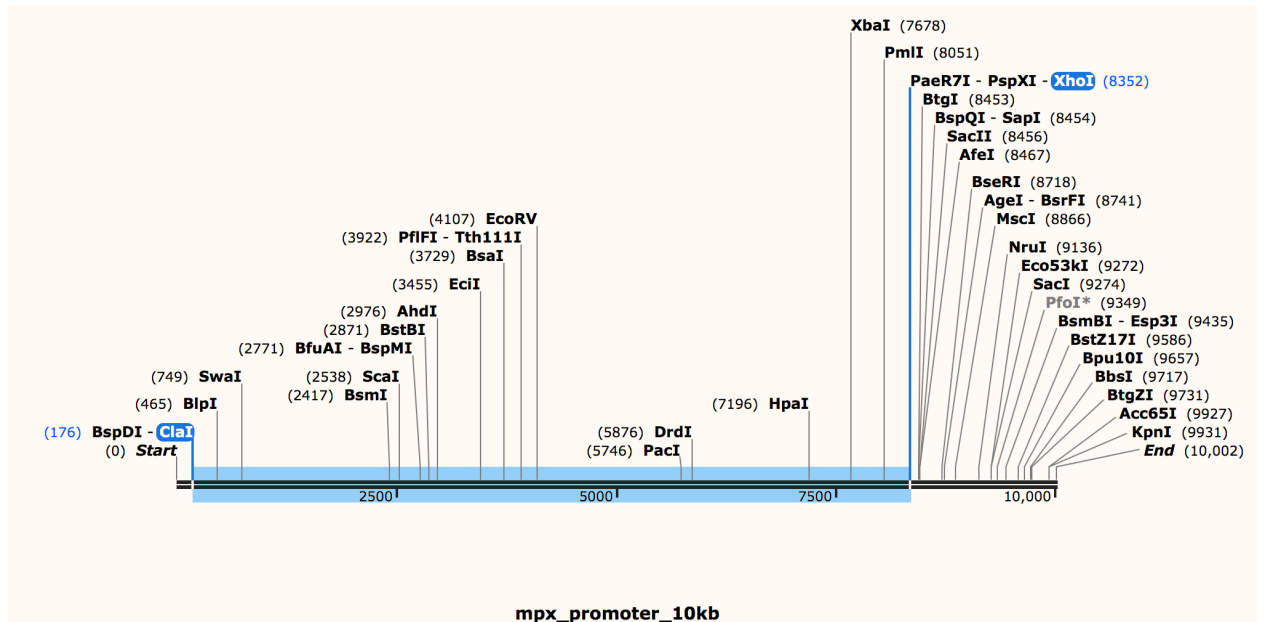


Figure 11: Restriction enzyme map of 10,000 bp region upstream of *mpx* in the GRCz11 zebrafish genome assembly. The Tg(*mpx*:EGFP) reporter line used an 8,177 bp region between the ClaI and XhoI restriction enzymes (highlighted in blue).

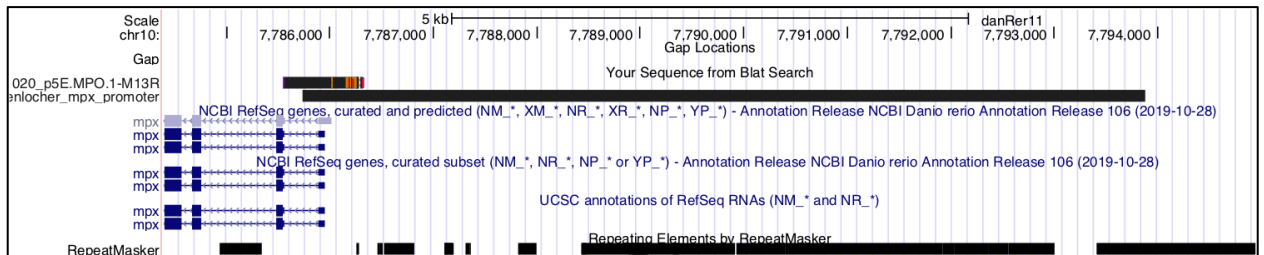


Figure 12: Alignment of the p5E-*mpx* clone and Huttenlocher *mpx* promoter sequence to the GRCz11 zebrafish genome assembly viewed in the UCSC Genome Browser. The p5E-*mpx* clone sequence aligns up to the start of the second exon. The two sequences were merged to generate a predicted promoter sequence from Chr. 10:7,785,544-7,793,885 that was 8,341 bp in length.

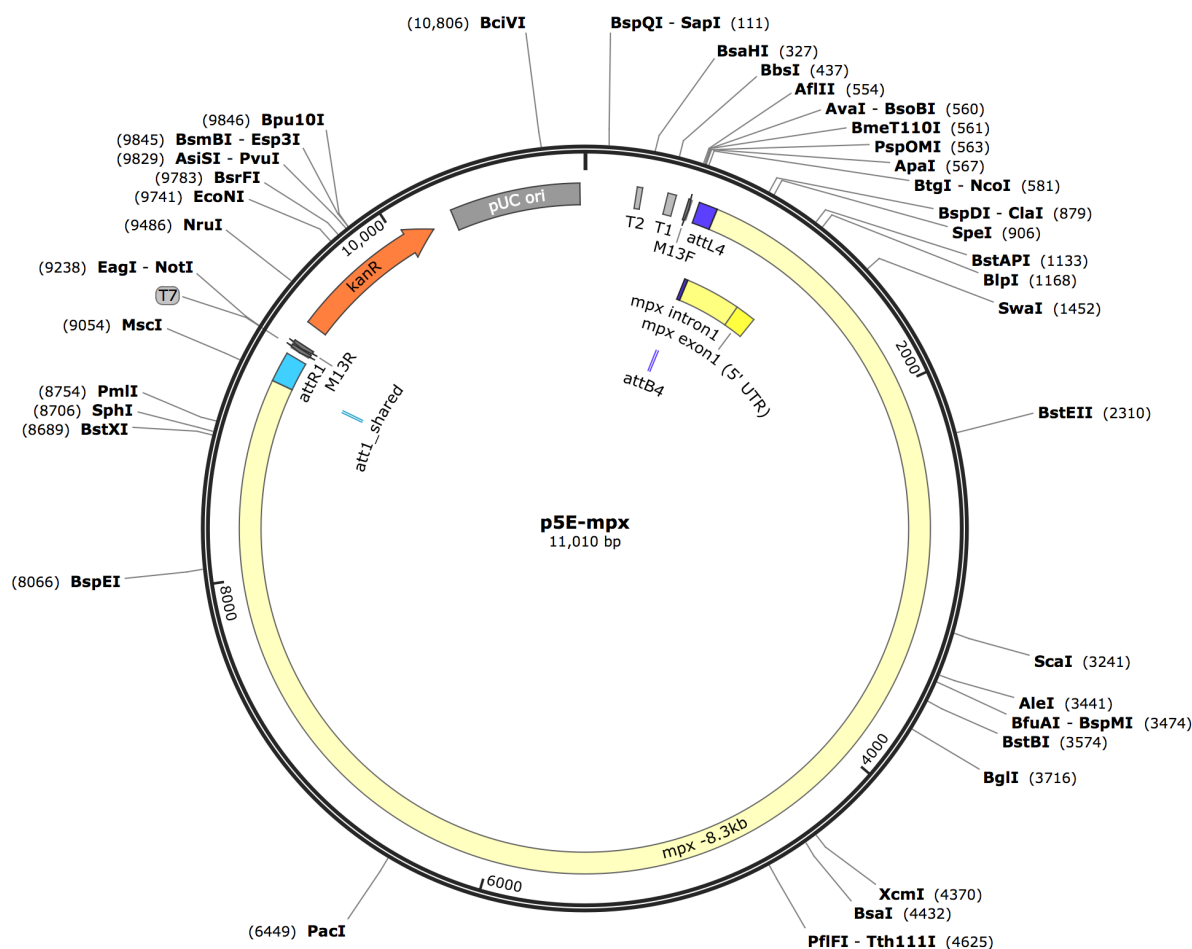


Figure 13: Circularized map of the predicted sequence of the p5E-*mpx* plasmid. This plasmid was developed by Jeremy Charette, of the Kim lab at the University of Maine. The predicted plasmid contains a total of 11,010 nucleotides, and contains the functional *mpx* promoter.

Middle entry clone containing the HyPer coding sequence (pME-HyPer)

The next step to create the Tg(*mpx*:HyPer) line was to generate a middle entry clone that containing the coding sequence (CDS) of reactive oxygen species biosensor, HyPer. The strategy was to insert the HyPer CDS into the pME-MCS donor plasmid using a BP Clonase II reaction. The BP Clonase II enzyme recombines PCR products that have attB sites and a donor vector that contains attP sites to generate an entry clone. The King Lab acquired a *actb*:HyPer plasmid from the Philipp Niethammer at Memorial Sloan Kettering

Cancer Center (Figure 14) (Enyedi 2013). Within the *actb*:HyPer plasmid, the HyPer coding sequence is located between attB1 and attB2 sites. The pME-MCS donor plasmid contained the attP sites.

The HyPer CDS from the *actb*:HyPer plasmid was amplified using PCR and a fragment of the PCR product was sequenced (Figure 15). The sequence of the product was identical to the sequence provided by the Niethammer Lab. We were unsuccessful in generating a pME-HyPer plasmid using a BP Clonase II reaction. However, we did create a sequence to represent the pME-HyPer plasmid (Figure 16). This sequence was created by editing the sequence of the pME-EGFP clone from the Tol2kit and replacing the EGFP CDS with the HyPer CDS.

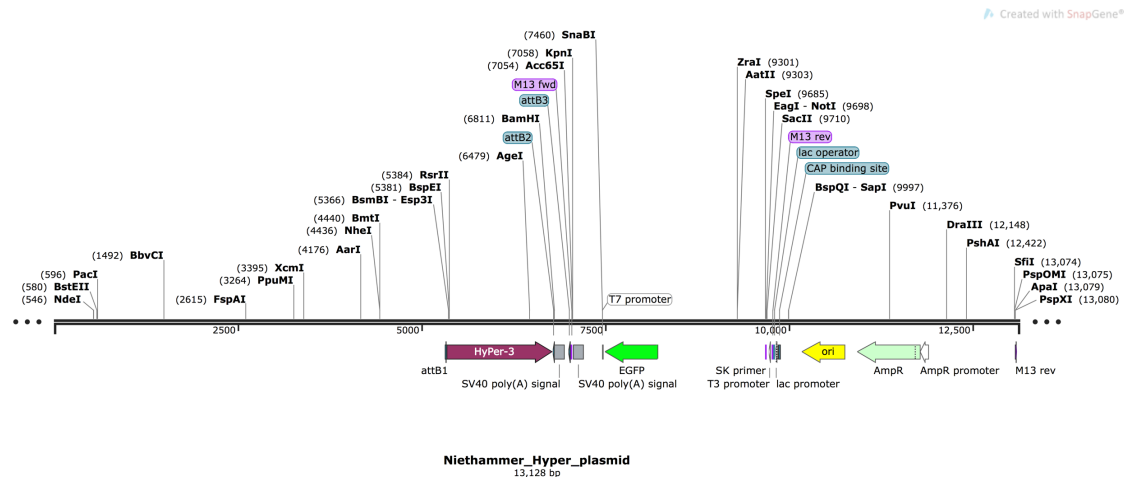


Figure 14: Circularized map of the *actb*:HyPer plasmid. The 13,128 bp plasmid sequence was provided by the Niethammer Lab. HyPer sequence shown to be properly located between attB1 and attB2 sites. Ampicillin resistance gene with associated promoter is located on right arm of plasmid.

Query	37	ACATGTCCTTGTCTGGAAGTTCGCTGATCCGGCCGCTCGGGATTCACTTCTCGGCATTGGA	96
Sbjct	5955	ACATGTCCTGTCTGGA-GTTC-GTACCC--GCCGC-CGGGAT-CACT-CTCGGCAT-GGA	6006
Query	97	CGAGCTGTAAACAACCTGGATG-CGGTAGCGCTGGCATCGGCAGCA-GGCGAGGAGCTG	154
Sbjct	6007	CGAGCTGTGA-CAAC-GTGTATGCGCGTAGCGCTGGCACCGCAGCAAGGCGAGGAGCTG	6064
Query	155	TTCAACCGGGGTGGTCCCCATCTCTGTGAGCTGGACGGCGACGATAAACGGGCCACAAG	214
Sbjct	6065	TTCAAC-CGGGTGGTGCC-ATCCTGTGTGAGCTGGACGGCGACGATAAACGG-CCACAAG	6121
Query	215	TTCAAGCTGTCTCGGCGAGGGGCGAGGCGCATGCCA-TACGGCAAGCTGACCTGAAGCT	27
Sbjct	6122	TTCAAGCTGTCTCGGCGAGGCG-CGAGGCGCATGCCACCTCTCGGCAAGCTGACCTGAAGCT	6180
Query	274	GATCTGCACACCGGCAAGCTGCCGTGCCCTGCCCTGACCCAGCTCGTGAACCTTCGGCTA	333
Sbjct	6181	GATCTGCACACCGGCAAGCTGCCGTGCCCTGCCCTGACCCAGCTCGTGAACCTTCGGCTA	6240
Query	334	CGGCGTGAAGTGCTTCGCCCGCTACCCGACACATGAAGCAGCAGACTTCTTCAAGTC	393
Sbjct	6241	CGGCGTGAAGTGCTTCGCCCGCTACCCGACACATGAAGCAGCAGACTTCTTCAAGTC	6300
Query	394	CGCCATGCCCGAAGGCTACGTCCAGGAGCGCACATCTTCTTCAAGGACGAGGCCAATA	453
Sbjct	6301	CGCCATGCCCGAAGGCTACGTCCAGGAGCGCACATCTTCTTCAAGGACGAGGCCAATA	6360
Query	454	CAACACACCGCGCGAGCTGAAGTTCGAGGGCACAACCTGTGGAACCGATCGAGCTGAA	513
Sbjct	6361	CAAGACCCGCGCGAGGTGAAGTTCGAGGGCGACACCTGTGAACCGCATCGAGCTGAA	6420
Query	514	GGGCACTCGGCTTCAAGGAGGACGGCAACATCTCGGGGACAAAGCTGGAGTACAACGGCAC	573
Sbjct	6421	GGGCACTCGGCTTCAAGGAGGACGGCAACATCTCGGGGACAAAGCTGGAGTACAACGGCAC	6480
Query	574	CGGTTTCGTTTTGAAGCGGGGCGGATGAAGATACACACTTCCGCGCGACACGCTTGG	63
Sbjct	6481	CGGTTTCGTTTTGAAGCGGGGCGGATGAAGATACACACTTCCGCGCGACACGCTTGG	6540
Query	634	AACCTGTGGCCAATGGTGGCGGCAGTAGCGGGATCACTTACTGCCACGCGTGGCTGT	693
Sbjct	6541	AACCTGTGGCCAATGGTGGCGGCAGTAGCGGGATCACTTACTGCCACGCGTGGCTGT	7000
Query	694	GGCGCGGAGCGACAAGCGCGATGGGTTGTTTATCTCGCGCTCAATTAAGCGGAACACG	753
Sbjct	6601	GGCGCGGAGCGACAAGCGCATGGGTTGTTTATCTCGCGCTCAATTAAGCGGAACACG	7660
Query	754	CGCACTATTGGCGTGTTTATCGTCTGGCTCACCGCTGCGACGCGCATGAGCAAGCT	813
Sbjct	6661	CGCACTATTGGCGTGTTTATCGTCTGGCTCACCGCTGCGACGCGCATGAGCAAGCT	6720
Query	814	GGCAGAGGCCATCCGCGCAAGATGGATGCCATTTCGATAAAGTTTAAACAGCGCGGT	873
Sbjct	6721	GGCAGAGGCCATCCGCGCAAGATGGATGCCATTTCGATAAAGTTTAAACAGCGCGGT	6780
Query	874	TTAACACCAGCTTCTCTGTACAAGATGGGGGATCCAGACATGATGAAGATACATTGATGA	933
Sbjct	6781	TTAACACCAGCTTCTCTGTACAAGATGGGGGATCCAGACATGATGAAGATACATTGATGA	6840
Query	934	GTTTGACAACAACCAACTAGAATGCAGTGAAAAAATGCTTTATTGTGAAATTTGTGA	993
Sbjct	6841	GTTTGACAACAACCAACTAGAATGCAGTGAAAAAATGCTTTATTGTGAAATTTGTGA	6900
Query	994	TGCTATTGCTTTATTTTGTAACCATTTAAGCTGCAATAAACAGTTAAACAAGAGACAAAT	1053
Sbjct	6901	TGCTATTGCTTTATTTTGTAACCATTTAAGCTGCAATAAACAGTTAAACAAC--ACAAT	6958
Query	1054	TGCATTCATTTATGTTTTCAGGTTCCAGGGGAGGTGTGGAGG-TTTTTCCACTTTATT	1112
Sbjct	6959	TGCATTCATTTATGTTTTCAGGTTCCAGGGGAGGTGTGGAGGTTTTTTCACATTTATT	7018
Query	1113	AAAC 1116	
Sbjct	7019	ATAC 7022	

Figure 15: Pairwise BLASTN alignment of a 1,121 nucleotide sequence of the PCR amplified LR(actb:HyPer) plasmid sequence provided by the Niethammer Lab. The coordinates for the HyPer sequence in the plasmid are 5,348-6,784 (indicated in blue). The alignment was 97% identical over 1,084 bp.

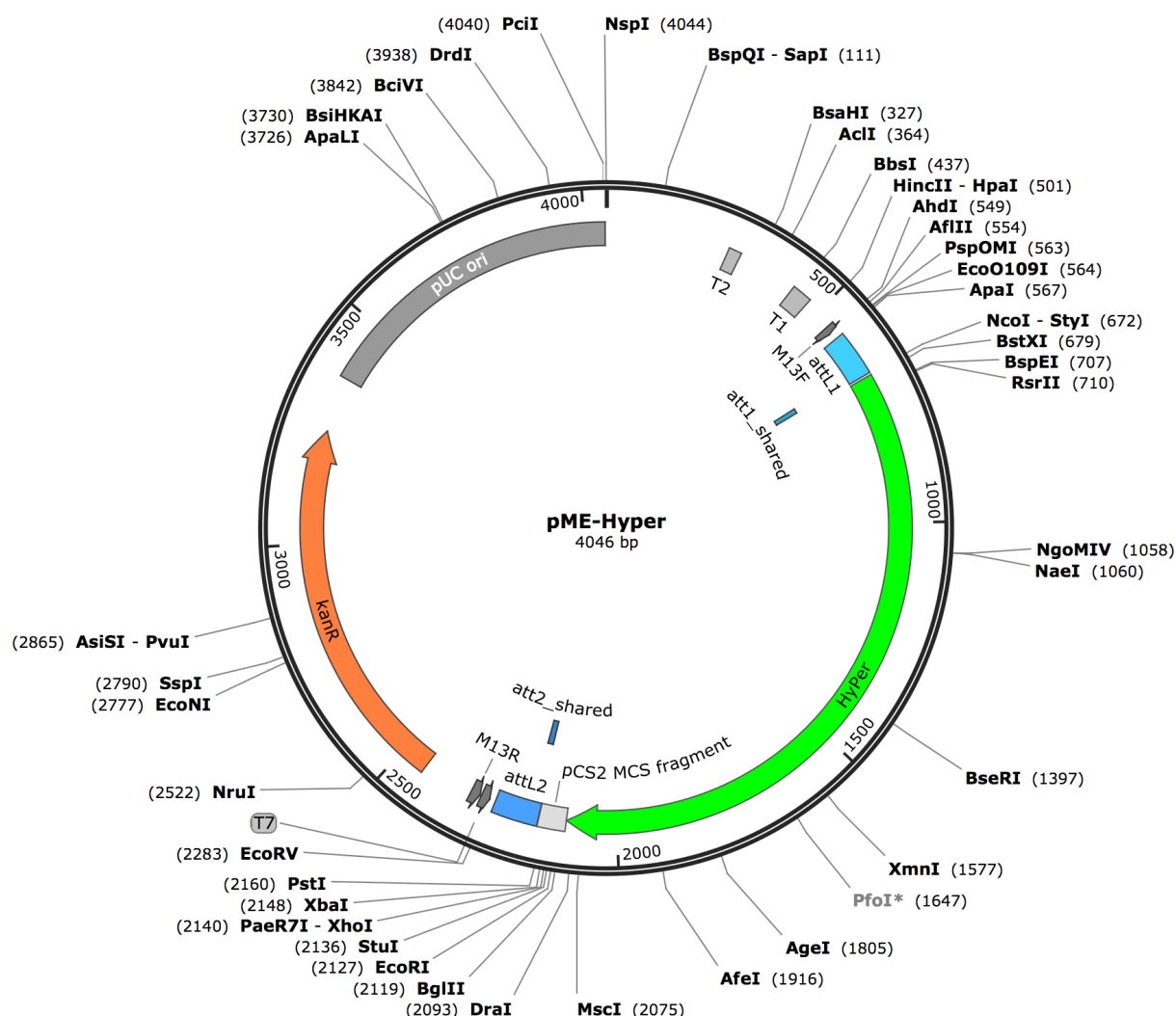


Figure 16: Circularized map of the predicted sequence of the pME-Hyper plasmid. This 4,046 bp sequence was generated by substituting the EGFP coding sequence with the HyPer coding sequence from the Niethammer actb:HyPer plasmid shown in Figure 14.

3p entry clone containing a polyA sequence (p3E-polyA)

The 3p-entry clone that was to be used in the final vector assembly by LR Clonase reaction was the p3E-polyA sequence provided in the Tol2Kit (Figure 17). Clones of this plasmid were cultured under the selective pressure of the antibiotic kanamycin. In the final vector assembly, this entry clone contains a polyA sequence that is required for HyPer

expression. A polyA sequence was engineered in the *actb*:HyPer plasmid from the Niethammer Lab (see Figure 14).

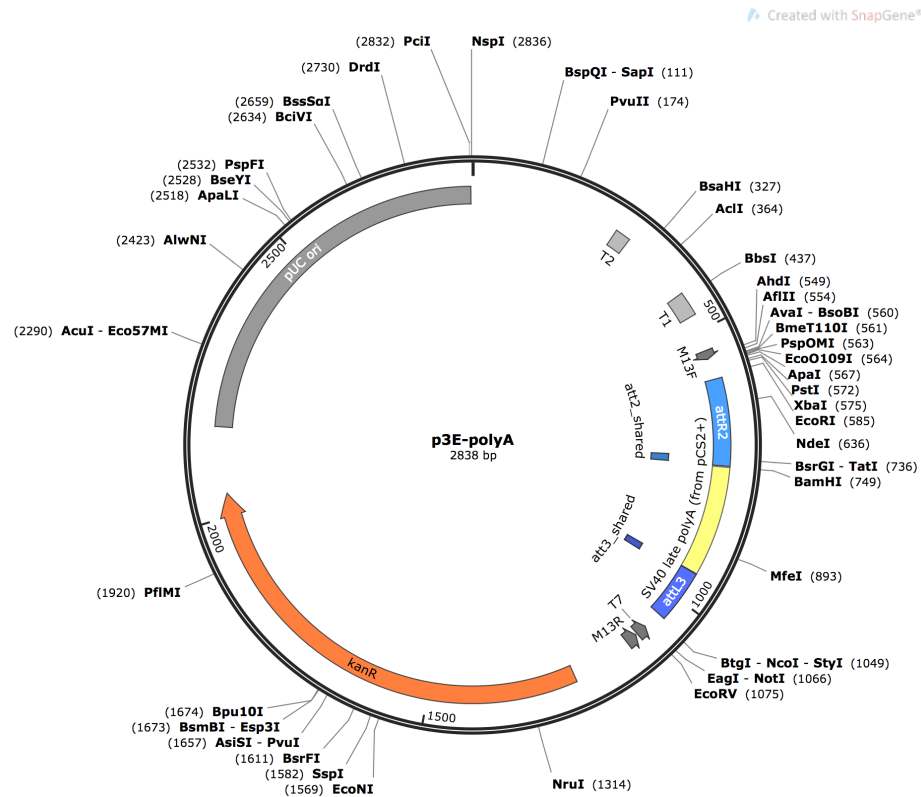


Figure 17: Circularized plasmid map of 3' entry vector used in final vector assembly. This 2838 nucleotide 3' entry vector contains a SV40 polyA sequence. This p3E-polyA plasmid was provided in the Tol2 kit.

Destination vector (pDestTol2pACryGFP)

The destination vector planned that was to be used in the generation of the final vector assembly was pDestTol2pACry (Figure 18) (Berger 2013). This plasmid was obtained from AddGene. This plasmid was designed to express GFP in the lens of zebrafish using an alpha-crystallin (*cryaa*) promoter. Expression of GFP in the lens will allow for rapid screening of embryos that express the *mpx*:HyPer transgene.

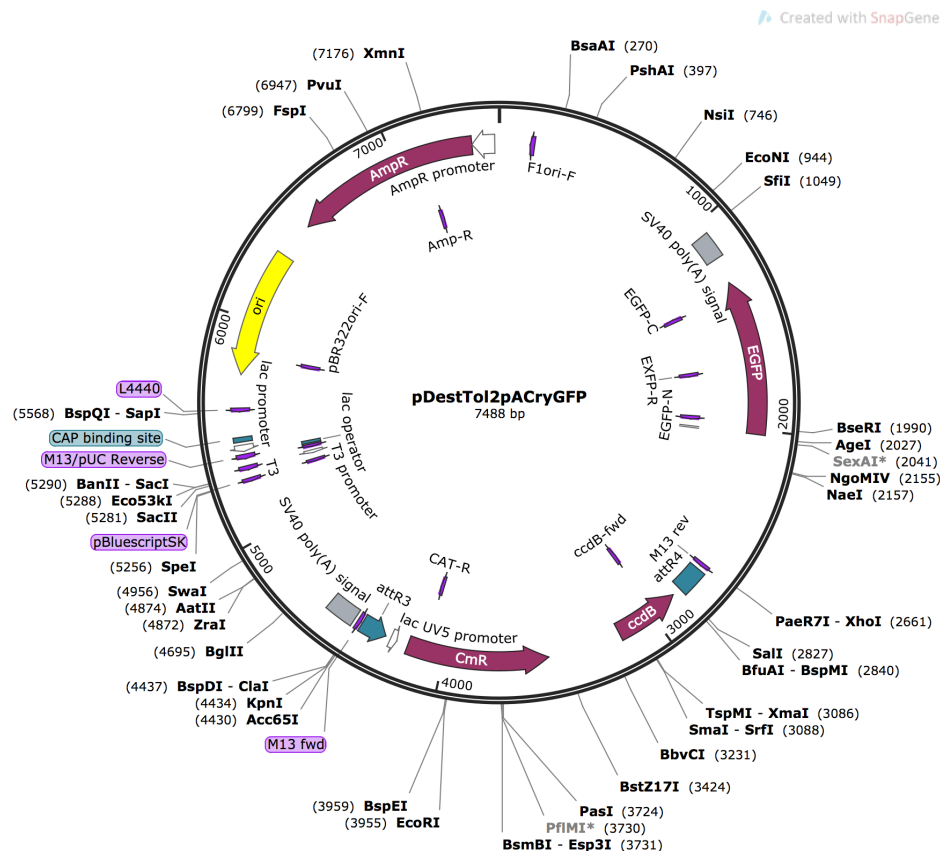


Figure 18: Circularized plasmid map of the pDestTol2pACryGFP destination vector. This destination vector was obtained from AddGene and is utilized for final vector assembly and screening transgenic zebrafish. Within this plasmid, there is a GFP encoding sequence following an *cryaa* promoter.

Predicted plasmid design

The final vector assembly would be generated using the 5p, 3p, and middle entry vectors with the destination vector. This vector would be assembled through an LR Clonase reaction of the four components. Ideally this vector would be assembled in the proper orientation with the 5p entry vector containing the *mpx* promoter ahead of the HyPer coding sequence provided in the pME-HyPer sequence followed by the poly A sequence of the 3p entry vector. Using the A Plasmid Editor (ApE) software, we generated a predicted final vector sequence from the LR reaction (Figure 19).

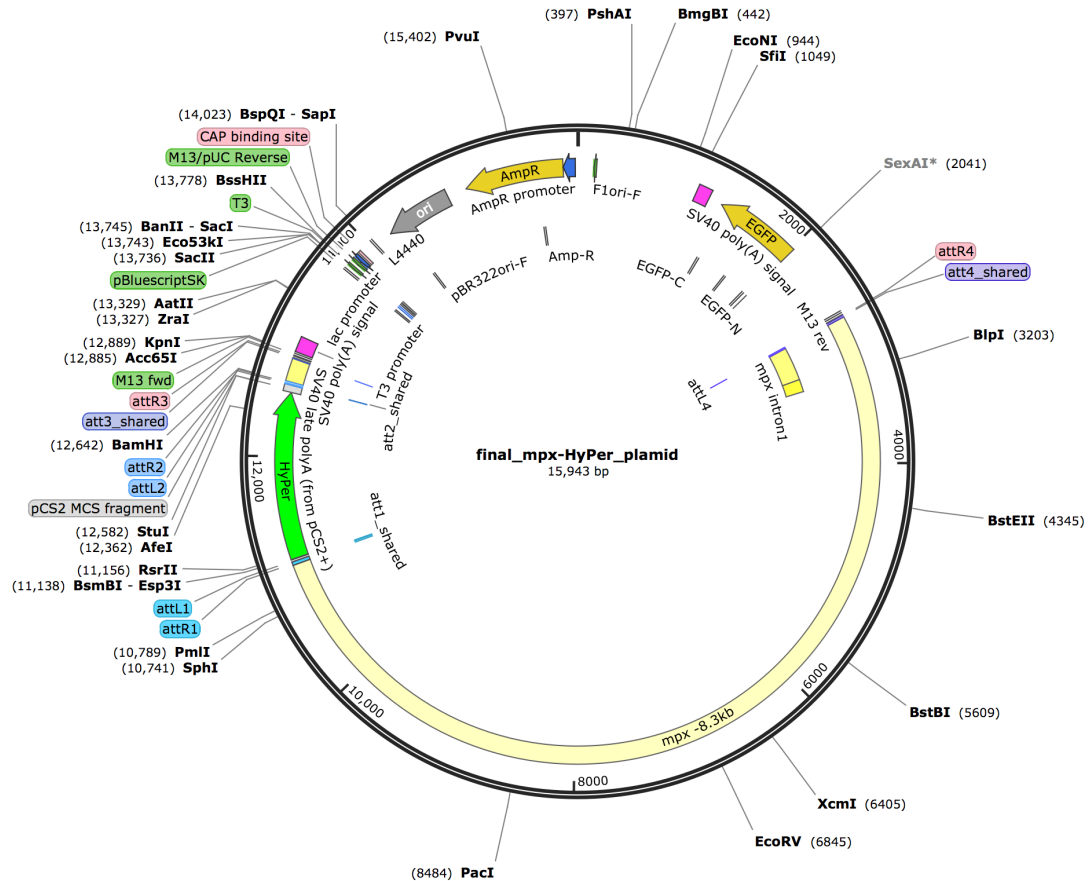


Figure 19: Predicted final plasmid sequence. Using the ApE software, a using the p5E-mpx, pME-HyPer, p3E-polyA, and Tol2 destination vector, pDestTol2pACryGFP using LR Clonase. The plasmid is expected to contain the 8.3kb *mpx* promoter, 1.5kb HyPer coding sequence and an Ampicillin resistance gene.

Expression of innate immune system genes associated with ROS

The response of the innate immune system to infection and/or injury is a dynamic process that involves the regulation of gene expression. The expression of a total of five genes in 48 hpf embryos injected with HBSS or IAV at time points ranging from 0 to 120 hours post infection (hpi) was assayed by qRT-PCR. NADPH oxidase 2 (*cybb*) was significantly upregulated at 18, 24, and 96 hpi (Figure 20A). Neutrophil cytosolic factor 1 (*ncf1*) was significantly upregulated at 12, and 36 hpi, and significantly downregulated at 18 hpi (Figure 20B). Nuclear factor erythroid 2-related factor 2 (*nfe2l2a*) was significantly

downregulated at 12 and 72 hpi, and significantly upregulated at 24, and 120 hpi (Figure 20C). The expression of alpha-1 antitrypsin (*serpinal*) was significantly increased at 18 hpi (Figure 20D). Superoxide dismutase 1 (*sod1*) was significantly downregulated at 3 and 6 hpi (Figure 20E).

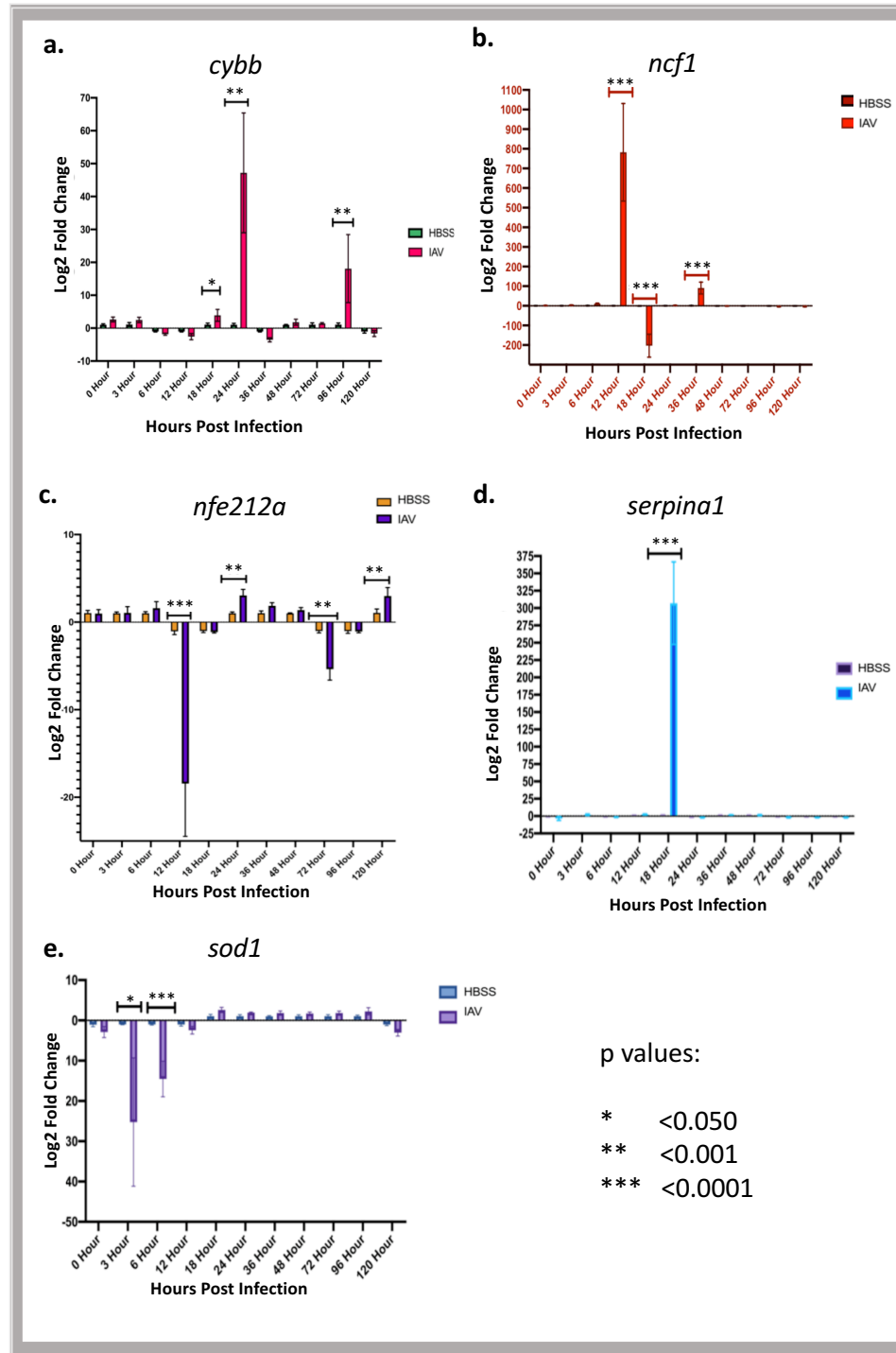


Figure 20: Expression of *cybb*, *ncf1*, *nfe2l2a*, *serpin1*, and *sod1* during IAV infection from 0-120 hpi. Log₂ fold change of candidate genes at 0, 3, 6, 12, 18, 24, 36, 48, 60, 72, 96, and 120 hpi ($n = 3$) comparing HBSS injected and IAV infected 48 hpf zebrafish embryos. The expression of beta-actin (*actb*) was used to normalize gene expression levels in all samples. (A) The expression of *cybb* was significantly upregulated at 18, 24, and 96 hpi. (B) The expression of *ncf1* was upregulated at 12, downregulated at 18 hpi, and upregulated again at 36 hpi. (C) The expression of *nfe2l2a* was downregulated at 12 hpi, upregulated at 24 hpi, downregulated at 72 hpi, and upregulated at 120 hpi. (D) The expression of *serpin1* was upregulated at 18 hpi. (E) The expression of *sod1* was downregulated at 3, and 6 hpi.

DISCUSSION

Development of the Transgenic Zebrafish Model:

The long term goal of this project was to develop a new transgenic zebrafish fluorescent reporter line, Tg(*mpx*:HyPer), to visualize ROS generated by neutrophils. This model would express the HyPer protein, a ROS biosensor, specifically in neutrophils. This biosensor fluoresces at differential wavelengths dependent on the concentration of ROS. This model could be used to study the inflammatory response to viral, bacterial, or fungal infection, or with injury.

Founders for the transgenic line would have been created by coinjection of the final plasmid vector and the Tol2 transposase into fertilized zebrafish embryos. The final vector would have been generated using multisite Gateway cloning where a LR Clonase reaction would assemble the three entry vectors and a singular destination vector. Prior to the final vector assembly, the middle entry clone, pME-HyPer, would need to be generated using a BP Clonase reaction. The final plasmid vector that was designed was approximately 15.9kb in length (Figure 19). Following microinjections, visual screening of potential transgenic positive zebrafish would occur at 2 dpf by observing GFP expression in the eyes of embryos. Once these transgenic embryos develop into adult zebrafish, these founders are bred to create a stable transgenic line after multiple generations. Embryos from these adults can be used to study ROS generated by neutrophils in the context of infection or injury.

The design of the Tg(*mpx*:HyPer) transgenic line uses the promoter for *mpx* to drive expression of HyPer in neutrophils. We don't know if *mpx* is the most efficient promoter by which to express HyPer in neutrophils. Lysozyme C (*lysc*) is another gene that is highly expressed in neutrophils. Using the promoter for *lysc* is another potential way to drive the

expression of HyPer in neutrophils (Figure 5). It may turn out using a *lysc* promotor may prove to be more efficient. The overall process of designing a Tg(*lysc*:HyPer) transgenic line would be the same, but a different entry clone (p5E-*lysc*) would need to be developed and used in the multisite LR Clonase reaction.

Development of the pME-HyPer entry clone from the BP reaction:

This project was stalled during the development of the pME-HyPer entry clone. This plasmid was to be generated through a BP Clonase II reaction where the HyPer sequence from the Sloan-Kettering plasmid would have been cloned into the pME-MCS plasmid from the Tol2 kit. We believe that the BP reaction did not work due to the primers used to amplify the HyPer coding sequence that was flanked by the attB sites. We made several attempts to complete the BP reaction, but the product of those reactions did not resemble the expected plasmid entry vector shown in Figure 16. A different primer design should make it possible to create the correct pME-HyPer plasmid.

Differential Gene Expression in Response to Infection:

Using qRT-PCR we evaluated the differential expression of five genes known to be associated with the respiratory burst response. NADPH oxidase 2 (*Cybb*) is the primary protein that is responsible for the generation of reactive oxygen species. (Figure 2). Neutrophil cytosolic factor 1 (*ncf1*) encodes the p47 protein which is a part of the Nox2 complex, regulating neutrophil activity. Nuclear factor erythroid 2-related factor 2 (*nfe2l2a*) encodes a transcription factor used to regulate the transcription of antioxidant proteins which protect tissues from damage. Alpha-1 antitrypsin (*serpina1*) transcription

is regulated by Nfe2l2a, and plays a role in preventing tissue damage from inflammation-related enzymes. Superoxide dismutase 1 (*sod1*) is also regulated by Nfe2l2a, and is used to render superoxide inert by breaking down the molecules. The expression of these five genes were evaluated relative to beta-actin across a total of 11 time points from 0hpi to 120hpi following injection of HBSS or infection from IAV.

Using the qRT-PCR results of relative expression, we can begin to theorize potential regulatory interactions among some of the genes. The most promising connection is between the *ncfl* and *nfe2l2a* expression levels at 12 hpi. The expression of *ncfl* was increased while the expression of *nfe2l2a* was decreased. NFe2l2a is a transcription factor that regulates the expression of antioxidant proteins which protect tissues from damage. *ncfl* encodes a subunit of the Cybb complex that produces ROS. At 12 hpi, the transcription factor responsible for repressing the effect of ROS, *nfe2l2a*, is downregulated, while there is increased expression in a component of the NADPH oxidase complex. This inverse correlation suggests that at 12 hpi, there is an inverse correlation of expression of a gene enabling ROS containing molecules to be produced, and genes that needed to protect against ROS damage.

There is also a potential for inverse correlation between *ncfl* and *serpinal* at 18hpi. The Serpinal1 protein also reduces tissue damage from inflammation. At 18hpi, *ncfl* had decreased expression and *serpinal* had increased expression. The inverse correlation between *ncfl* and *serpinal* at 18 hpi was opposite of what was observed with *ncfl* and *nfe2l2* at 12 hpi. In that relationship, *ncfl* had increased expression and *nfe2l2* had decreased expression. These two inverse correlations suggest that there is feedback

between the utilization of ROS by the innate immune system and genes that need to be expressed to limit damage to zebrafish tissues during the course of infection.

While the results from the qRT-PCR can be used to make some proposed regulatory interactions between the different genes associated with the respiratory burst response, there are some limitations of the experimental data. For one, qRT-PCR assays the RNA present in a sample, and not the protein levels. It is possible that the expression at the RNA level is completely different than that of the protein. Post translational regulation of proteins can also effect the actual amount of protein present at any one time. Furthermore, we assayed gene expression using RNA extracted from three whole embryos per sample. Three embryos were used to obtain enough RNA for the cDNA synthesis needed for the qRT-PCR assays. Each of the individual zebrafish may have had varying expression levels over the course of infection. This variation is lost by pooling the three embryos together. We also assayed RNA from whole embryos and not just phagocytes. Ideally, we want to understand the expression of these respiratory burst related genes in the context of neutrophils.

Future Applications of the Tg(*mpx*:HyPer) Zebrafish Line:

Following its development, this zebrafish line will be a powerful tool for studying innate immunity *in vivo*. Zebrafish are used to study host-pathogen responses to bacterial, fungal and viral infection. At 4 dpf, localized infection of the swim bladder may be performed to study detect the levels of ROS associated with neutrophils in these host-pathogen interactions. Furthermore, responses to injury can also be studied. We believe that the immunological responses observed in this model can be translated to humans.

The ability to cross this line with other zebrafish lines will further research on innate immunity. Once developed, the Tg(*mpx:HyPer*) line can be crossed with various other zebrafish models to study additional immunological reactions to injury or infection. For example, this line could be crossed with the Tg(*mpeg1:mCherry*) line that expresses mCherry in macrophages. In another example, this model can be crossed with the WHIM (Tg1(-8*mpx:cxc4b-EGFP*)) model, that possesses defective neutrophils, to observe the change in the respiratory burst response with defective neutrophil trafficking.

The Tg(*mpx:HyPer*) model could be used to study the function of specific genes by knocking down genes using morpholinos. Morpholinos can be used to knockout a targeted gene over the first five days of development. Studies of morphants could reveal differences in H₂O₂ in response to infection. One gene of interest would be *ncfl* as it has a known role in the respiratory burst response. New research by Lily Charpentier and Brandy Soos in the King Lab show that *ncfl* morphants have increased survival following IAV infection. Knocking down *ncfl* in the Tg(*mpx:HyPer*) model would allow us to visualize any changes in H₂O₂ production in localized infection.

Following the development of this model, the respiratory burst response and the roles of reactive oxygen species may be further understood. This includes the many regulatory factors and feedback loops that are part of the innate immune response to injury or infection. Using this model, we may be able to test different small molecules that alter the ROS production during an IAV infection thereby optimizing the response to IAV. Any small molecules found could eventually become new treatments for IAV infection. For example, the drug Ebselen and other ebselen-sulfur analogs are known to inhibit Cybb (Sorce 2017). Cybb is the primary protein required for ROS production and inhibition of

Cybb would lead to a less robust respiratory burst response. Even though there may be a diminished response to IAV, it could stop a hyperinflammatory response that would otherwise lead to tissue damage. Similar small molecule screens could be performed to find new therapeutics for bacterial and fungal infections, and enhance responses to injury.

REFERENCES

- Belousov V., *et al.* Genetically encoded fluorescent indicator for intracellular hydrogen peroxide. *Nature Methods*. (2006) 3(4):281-286 DOI:10.1038/NMETH866.
- Berger, J., Currie PD. 503unc, a small and muscle-specific zebrafish promotor. *Genesis*. (2013) 51(6):443-447. PubMed 23444339.
- Dadonaite, B., *et al.* The structure of the influenza A virus genome. *Nature Microbiology*. (2019) 4:1781-1789.
- Dou, D., *et al.* Influenza A Virus Cell Entry, Replication, Virion Assembly and Movement. *Frontiers in Immunology*. (2018) 5(1581):1-17. doi: 10.3389/fimmu.2018.01581.
- Ellett, F., *et al.* *mpeg1* promotor transgenes direct macrophage-lineage expression in zebrafish. *Blood*. (2011) 117(4): e49-e56. PMID: 21084707.
- Enyedi, B., Niethammer, P. H₂O₂: A Chemoattractant. *Methods in Enzymology*. (2013) 528:237-255. doi: 10.1016/B978-0-12-405881-1.00014-8.
- Freisinger, C., Huttenlocher A. Live Imaging and Gene Expression Analysis in Zebrafish Identifies a Link between Neutrophils and Epithelial to Mesenchymal Transition. *PLoS ONE*. (2014) 9(11):1-14. DOI: 10.1371/journal.pone.0112183
- Fukuyama, S., *et al.* Multi-spectral fluorescent reporter influenza virus (Color-flu) as powerful tools for *in vivo* studies. *Nature Communications*. (2015) 1-8. DOI: 10.1038/ncomms7600
- Gabor, KA., *et al.* Influenza A virus infection in zebrafish recapitulates mammalian infection and sensitivity to anti-influenza drug treatment. *Disease Models & Mechanisms*. (2014) 7: 1227-1237. doi:10.1242/dmm.014746.
- Kawakami, K. *Tol2*: a versatile gene transfer vector in vertebrates. *Genome Biology*. (2007) 8(Suppl 1):S7. doi:10.1186/gb-2007-8-S1-S7.
- Kwan K, *et al.* The Tol2kit: A Multisite Gateway-Based Construction Kit for *Tol2* Transposon Transgenic Constructs. *Developmental Dynamics*. (2007) 236:3088-3099. DOI 10.1002/dvdy.21343.
- Nayak, D., *et al.* Textbook of Influenza, Second Edition, Structure, disassembly, assembly and budding of influenza virus Part 3. *John Wiley & Sons, Incorporated*. (2013) 37-56.
- Niethammer, P., *et al.* A tissue-scale gradient of hydrogen peroxide mediates wound detection in zebrafish. *Nature*. (2009) 459(7249): 996-999. doi:10.1038/nature08119

Panday, A., *et al.* NADPH oxidase: an overview from structure to innate immunity-associated pathologies. *Cellular & Molecular Immunology*. (2015) 12:5-23

Pase, L., *et al.* *In Vivo* Real-Time Visualization of Leukocytes and Intracellular Hydrogen Peroxide Levels During a Zebrafish Acute Inflammation Assay. *Methods in Enzymology*. (2012). 506:135-156. DOI: 10.1016/B978-0-12-391856-7.00032-9.

Pase, L., *et al.* Neutrophil-Delivered Myeloperoxidase Dampens the Hydrogen Peroxide Burst after Tissue Wounding in Zebrafish. *Current Biology*. (2012) 22(19):1818-1824. PMID:22940471.

Punt, J., *et al.* Immunology Eighth Edition. *Macmillan Learning*. (2019). 113-163. ISBN-13: 978-1-4641-8978-4.

Sorce S., *et al.* NADPH oxidases as drug targets and biomarkers in neurodegenerative diseases: What is the evidence?. *Free Radical Biology and Medicine*. (2017) 112: 387-396.

Watanabe T., *et al.* Cellular Networks Involved in the Influenza Virus Life Cycle. *Cell Host & Microbe* (2010) 7: 427-439. DOI 10.1016/j.chom.2010.05.008.

Webster, R., *et al.* Textbook of Influenza, Second Edition, Immunology of influenza Part 5. *John Wiley & Sons, Incorporated*. (2013) 269-309.

Yamayoshi, S., *et al.* Current and future influenza vaccines. *Nature Medicine*. (2019) 25:212-220. doi: 10.1038/s41591-018-0340-z.

Yang, P., *et al.* The Oxidative Burst System in *Amphioxus*. *Amphioxus Immunity*. (2016)

Yoo, S., *et al.* Spatiotemporal photolabeling of neutrophil trafficking during inflammation in live zebrafish. *Journal of Leukocyte Biology*. (2011) 89(5):661-667. PMID: 21248150.

AUTHOR'S BIOGRAPHY

James T. Seuch was born in Stamford, Connecticut on April 24, 1998. He graduated from Trumbull High School and completed the program at the Trumbull Regional Agriscience and Biotechnology Center, focusing in Biotechnology. James majored in Biochemistry and Molecular & Cellular Biology at the University of Maine. There he worked in the King laboratory for 3 academic years.

Following graduation, James will be attending the University of Rochester, enrolled in the Biophysics, Structural, and Computational Biology Ph.D. program.